Biomaterials 32 (2011) 5187–5194

Contents lists available at ScienceDirect

Biomaterials

journal homepage: www.elsevier.com/locate/biomaterials

The performance of gadolinium diethylene triamine pentaacetate-pullulan hepatocyte-specific T1 contrast agent for MRI

Hyeona Yim [a,1], Su-Geun Yang [b,g,1], Yong Sun Jeon [c], In Suh Park [d], Mina Kim [b], Don Haeng Lee [b,e], You Han Bae [b,f], Kun Na [a,*]

[a] Department of Biotechnology, The Catholic University of Korea, Bucheon, Gyeonggi-do 420-743, Republic of Korea
[b] Utah-Inha DDS and Advanced Therapeutics, B-403 Meet-You-All Tower, Songdo Technopark, 7-50, Songdo-dong, Yeonsu-gu, Incheon 406-840, Republic of Korea
[c] Department of Radiology, Inha University College of Medicine, Incheon, 420-751, Republic of Korea
[d] Department of Pathology, Inha University College of Medicine, Incheon, 420-751, Republic of Korea
[e] Department of Internal Medicine, Inha University College of Medicine, Incheon, 420-751, Republic of Korea
[f] Department of Pharmaceutics and Pharmaceutical Chemistry, The University of Utah, 421 Wakara Way, Suite 318, Salt Lake City, Utah 84108, USA
[g] Clinical Research Center, School of Medicine, Inha University, 2F A-dong, Jeongseok Bldg., Sinheung-dong 3-ga, Jung-gu, Incheon 400-712, Republic of Korea

ARTICLE INFO

Article history:
Received 1 February 2011
Accepted 29 March 2011
Available online 10 May 2011

Keywords:
MRI
Liver cancer
Pullulan
T_1 contrast
Gadolinium
Hepatocyte-specific contrast agent

ABSTRACT

The magnetic resonance (MR) functionalities of pullulan-conjugated gadolinium diethylene triamine pentaacetate (Gd-DTPA-Pullulan) as a new hepatocyte-specific contrast agent were evaluated. Pullulan, which specifically accumulates on hepatocytes via asialoglycoprotein receptors, was chemically linked with Gd-DTPA. Gd-DTPA-Pullulan displayed three times greater contrast enhancement than Gd-DTPA-BMA (Omniscan®) in delayed MR imaging (MRI) on orthotopic rat hepatocarcinoma (HCC). This contrast effect lasted up to 24 h. In particular, Gd-DTPA-Pullulan displayed a discriminative MR contrast on the regenerative and malignant hepatic nodules sequentially observed during the progress of cirrhotic HCC. Approximately 50% of injected Gd-DTPA-Pullulan was eliminated via the hepato-biliary system. IC_{50} of Gd-DTPA-Pullulan on Chang liver cells was much higher than Gd-DTPA and Gd-DTPA-BMA (309.1 ± 11.2, 173.5 ± 15.5 and 49.4 ± 8.9 μM, respectively). Any significant toxicities of Gd-DTPA-Pullulan at the conventional dose on the rats weren't detected on histology studies. Gd-DTPA-Pullulan worked as a hepatocyte-specific MR contrast agent with increased MR functionalities and an acceptable safety profile setting the scene for future clinical trials.

1. Introduction

Presently, most cancer therapy, including diagnosis, location of metastases, drug regimens, and determination of surgical margin, is becoming more reliant than ever on imaging technologies [1,2]. Various imaging technologies such as ultrasound, CT, MRI and PET have been applied for cancer diagnosis and therapy. Among them magnetic resonance imaging (MRI) provides excellent in vivo imaging, especially for soft tissue contrast, with high spatial (<1 mm) and temporal resolution. However the need for more accurate detection of the full extent of malignant lesions incites the use of intravenous contrast agents. Especially, hepatic MRI still has substantial shortcomings in terms of discriminative analysis of liver lesions even though with help of contrast agents [3] and attempts made to resolve these issues have met with limited success [4]. The complexities of hepatic pathologies, which include HCC, metastases, fibrosis, cirrhosis, cysts, hemangioma, and fatty liver, require more functional contrast agents [5]. Liver metastases are another diagnostic challenge. The liver ranks second only to the lymph nodes as a common site of metastasis of cancers from other organs. The most common sites of primary malignancy that spread to the liver are colorectal carcinoma, gastric adenocarcinoma, breast cancer, and lung cancer. Malignant cells detach from the primary cancer and travel to the liver via the portal vein and then attached and grow independently. Hepatic metastases form multiple tiny nodules, some of which cannot be detected without contrast agents [6].

Enhanced contrast is usually achieved by the selective accumulation of gadolinium in regions of interest. Various attempts have been tried to get enhanced target-specific MR imaging by using nanomaterials (i.e., nanotube, dendrimer, liposome) [7–9], tumor-specific ligands (i.e., folate, antibody, lipopeptide) [10–12] and etc. Aime's group employed Gd-loaded apoferritin for tumor vessel imaging. Apoferritin functioned as a good vascular targeting

* Corresponding author. Tel.: +82 2 2164 4832; fax: +82 2 2164 4865.
E-mail address: kna6997@catholic.ac.kr (K. Na).
[1] These authors equally contributed to this work.

0142-9612/$ – see front matter © 2011 Elsevier Ltd. All rights reserved.
doi:10.1016/j.biomaterials.2011.03.069

agent which induced enhanced and prolonged contrast of the tumor. They reported ~ 30% contrast enhancement of tumors (after 5 h) in a mouse subcutaneous model [13]. However, these attempts seem to be far away from clinical trials, even though they shows good contrast efficacy than conventional gadolinium products display, and to date, the most prominent approach involves modifying gadolinium chelates with a tissue-specific targeting ligand [13–15].

The contrast agents for hepatic MRI have been technically divided by their functional properties and mechanism of hepatic uptake. These include non-specific extracellular gadolinium chelates that distribute in extracellular region such as vascular and cerebro-spinal fluids, hepatocyte-selective contrast agents that are taken up specifically by hepatocytes and partly excreted via hepato-biliary system, and reticuloendothelial system (RES)-specific contrast agents that are typically classified as a dextran-superparamagnetic iron oxide (SPIO) complex for T2 MR imaging [6,16].

Gadopentetate dimeglumine (Gd-DTPA, Magnevist®, Bayer Schering Pharma AG), gadodiamide (Gd-DTPA-BMA, Omniscan®, GE Healthcare), and gadobutrol (Gd-DO3A-butrol, Gadovist®, Bayer Inc.) are classified as non-specific extracellular gadolinium agents [17]. The major applications of these extracellular agents are vascular and cerebro-spinal MR imaging. These extracellular agents are also frequently used in liver MR imaging because they are inexpensive and can also show other abdominal organ lesions in addition to liver lesions. However these agents do not allow a sufficient time for MR imaging (especially for delayed hepatic imaging) to get an accurate diagnosis of hepatic lesions, because only 2 ~ 4% of the injected dose accumulates in the liver and rapidly passes in a minute. In these reasons, development of new hepatocyte-specific MR agent which can provide more accurate and discriminative MR imaging of the complicated hepatic lesions is major interests of science. Until recently, only gadobenate dimeglumine (Gd-BOPTA, MultiHance®, Bracco Diagnostics Inc.) and gadoxetate (Gd-EOB-DTPA, Eovist®, Bayer HealthCare Pharma) are clinically available hepatocyte-specific T_1 agents that produce substantial hepatic enhancement in delayed imaging scans, peaking at 40–120 min after dosing [6,18].

In the present study, we designed new hepatocyte-specific contrast agent. Gadolinium-diethylene triamine pentaacetic acid (Gd-DTPA) was chemically attached to pullulan (Gd-DTPA-Pullulan). Pullulan is a natural and nonionic polysaccharide containing repeat malto-triose units condensed through α-1,6 linkage [19]. Interestingly, pullulan shows a specific affinity for asialoglycoprotein receptors (Fig. 1), which are highly expressed on sinusoidal membranes of hepatocytes [19–21]. Yamaoka et al. reported that more than 40% of pullulan accumulates in the liver after an intravenous administration [21]. Gd-DTPA-Pullulan as a hepatocyte-specific gadolinium agent can overcome the shortcomings of Gd-DTPA which belongs to typical extracellular gadolinium agents. MR sensitivities of Gd-DTPA-Pullulan were proved on a phantom study. Enhancement of MR contrast and sensitivity of Gd-DTPA-Pullulan were evaluated on a delayed MR imaging in an orthotopic rat HCC model and an N-diethylnitrosamine (DEN) induced rat cirrhotic HCC model. Acute toxicities of Gd-DTPA-Pullulan based on the cell viability studies, tissue histology and blood protein levels were estimated, and excretion pathway of Gd-DTPA-Pullulan was compared with Gd-DTPA-BMA on the rats.

2. Materials and methods

2.1. Materials

The neutral polysaccharide pullulan (MW 100,000) was acquired from Tokyo Chemical Industry Co., Ltd. Diethylene triamine pentaacetic dianhydride and $GdCl_3 \cdot 6H_2O$ were purchased from Sigma–Aldrich (St. Louis, MO, USA). Gd-DTPA-Pullulan was synthesized based on the reported methods [22,23], dialyzed and then lyophilized. Gadolinium contents of Gd-DTPA-Pullulan were estimated using inductively coupled plasma-optical emission spectrometry (ICP-OES) (SPECTRO GENESIS, Spectro Analytical Instruments GmbH, Germany). Gd-DTPA-BMA was used as a control MR agent. Chang Liver cells were acquired form from American Type Culture Collection (ATCC CCL 13, USA). All other chemicals were of analytical reagent grade and were used without further purification.

2.2. Synthesis of Gd-DTPA-Pullulan

Gd-DTPA-Pullulan was synthesized using the following method (Fig. S1, see supporting information). 300 mg of DTPA dianhydride and 150 mg of pullulan were dissolved in 80 ml of dry dimethylene sulfoxide (DMSO) and allowed to stand for 24 h at room temperature. Distilled water was then added gradually under magnetic stirring for 30 min, and the solution was dialyzed for 3 days and lyophilized (Fee-Zone 4.5, Labconco, Kansas, Mo). Subsequently, DTPA-pullulan and 0.6 mM $GdCl_3 \cdot 6H_2O$ were dissolved in 25 ml of water at 1:0.7 molar ratio of Gd to DTPA, titrated to pH 7.0 using 1 N NaOH, and stirred for 24 h to obtain stable Gd-DTPA chelation [22,23]. Gd-DTPA conjugated pullulan was acquired via dialyzing and lyophilizing this solution. Gadolinium contents were estimated on an inductive coupled plasma-optical emission spectrometry (Spectro Genesis, Spectro Analytical Instruments GmbH, Germany). The conjugation of DTPA to pullulan was confirmed via fourier transform infrared spectrometry (FT-IR) on a Nicolet Magna 550 series II (Midac, Atlanta, GA). Spectra was recorded on KBr plates over the range 4000 ~ 400 cm^{-1} at a wavenumber resolution of 2 cm^{-1}.

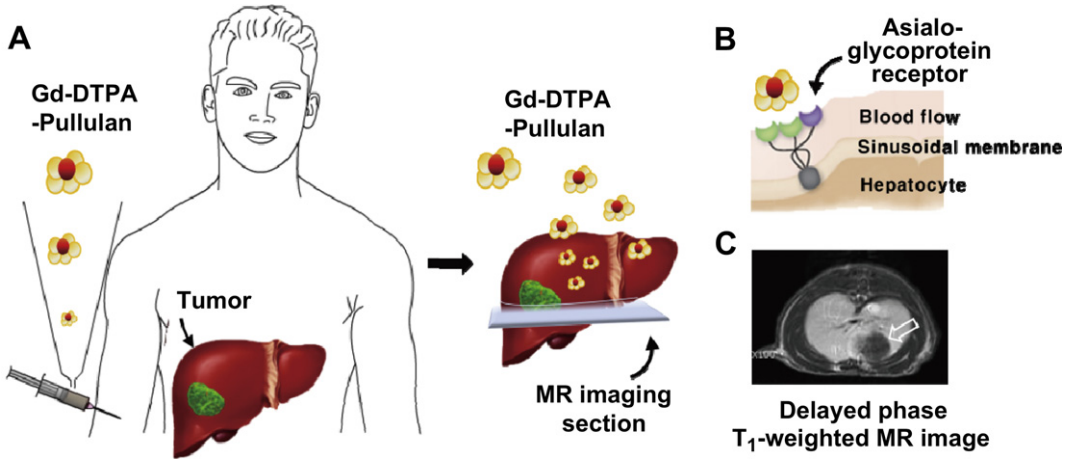

Fig. 1. A, schematic illustration of Gd-DTPA-Pullulan (Gd-DTPA-Pullulan) as a hepatocyte-specific MR agent. B, proposed uptake mechanism of Gd-DTPA-Pullulan by hepatocytes via asialoglycorotein receptors, wherein positive contrast was generated. C, typical T_1-weighted MR image of rat bearing N1S1 orthotopic HCC after an I.V. injection of Gd-DTPA-Pullulan, Gd-DTPA-Pullulan generates the enhanced positive contrast of normal hepatic parenchyma and allows the elongated MR diagnostic time window for up to 24 h after an injection.

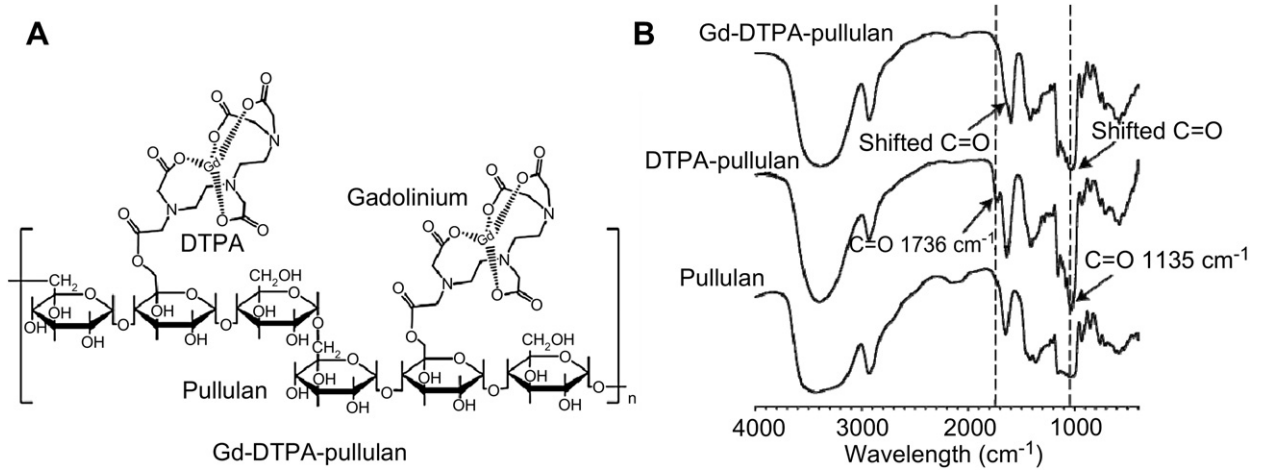

Fig. 2. A, chemical structure of Gd-DTPA-Pullulan. B, FT-IR spectra of pullulan, DTPA-pullulan, Gd-DTPA-Pullulan, the shifted C═O peak at 1736^{-1} suggests the successful conjugation and chelation of DTPA and Gd on pullulan.

2.3. Estimation of paramagnetic properties of Gd-DTPA-Pullulan

MRI experiments were conducted on a 1.5 T horizontal scanner (Signa Excite; GE Healthcare, Milwaukee, WI, USA) using a Litz coil (diameter 100 mm, length 85 mm, DOTY Scientific Inc., NC) at room temperature.

In vitro paramagnetic properties of Gd-DTPA-Pullulan were estimated on a phantom. Gd-DTPA-Pullulan solutions with 0, 0.5, 0.05, 0.005, and 0.0005 mM of gadolinium were added to the wells of a 12 well plate and introduced into a 1.5 T horizontal scanner (fast spin echo, TR = 400.0 ms, TE = 10.0 ms). GD-DTPA-BMA was selected as a T_1 reference and scanned under the same conditions as Gd-DTPA-Pullulan.

2.4. Establishment of animal HCC models

2.4.1. N1S1 implanted orthotopic HCC in rats

Male Sprague Dawley rats were purchased from Orient Bio, Inc. (Ga-pyeong, Kyoung-gi, Korea). All rats were provided food (Sam Yang Company, Seoul, Korea) and water ad libitum, maintained in a light-controlled room, and kept at

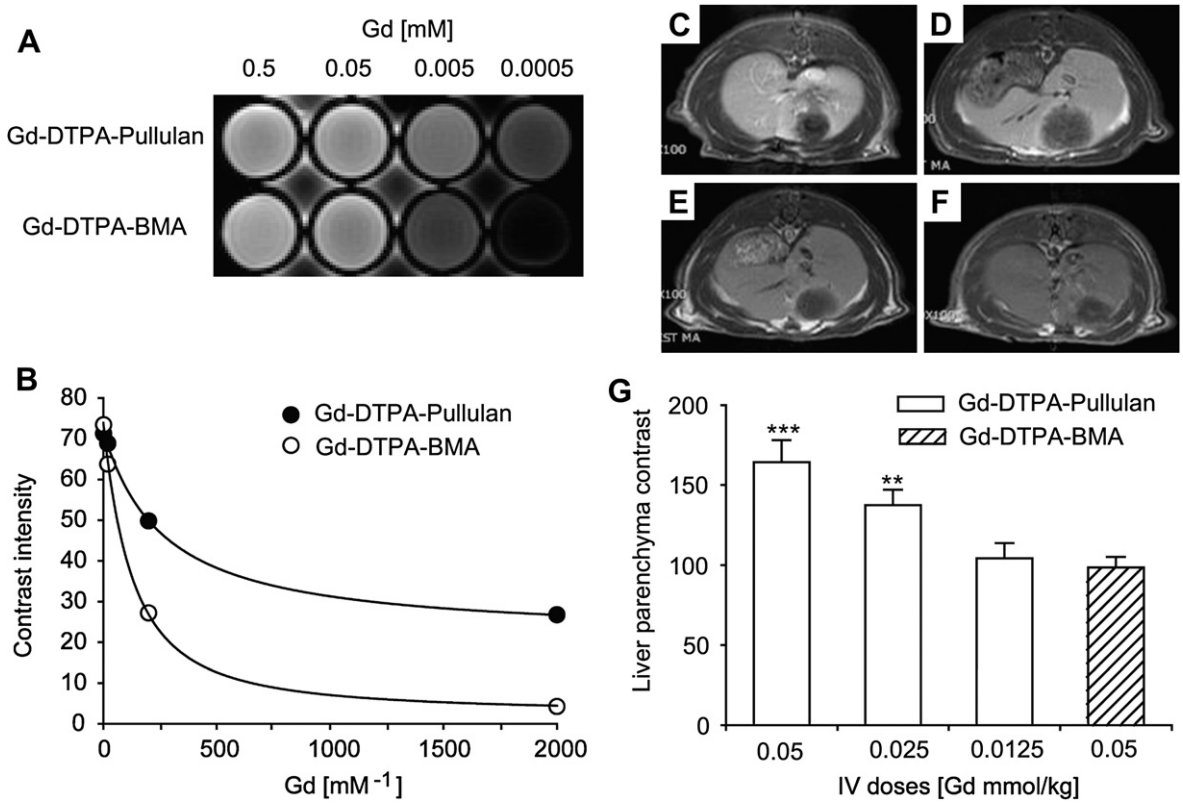

Fig. 3. *In vitro* and *in vivo* paramagnetic properties of Gd-DTPA-Pullulan in comparison with commercial product (Gd-DTPA-BMA, Omniscan®). A, T_1-weighted MR images of Gd-DTPA-Pullulan and Gd-DTPA-BMA solutions (1.5 T, TR = 400.0 ms, TE = 10.0 ms). B, *in vitro* contrast intensities of Gd-DTPA-Pullulan and Gd-DTPA-BMA solutions, Gd-DTPA-Pullulan displayed much higher bright contrast (higher contrast intensities) than Gd-DTPA-BMA. C, D, E, and F: Transverse T_1-weighted MR images 1 h after intravenous injection of 0.05, 0.025, or 0.125 mmol Gd/kg of Gd-DTPA-pullulan (A, B, and C) and 0.05 mmol Gd/kg of Gd-DTPA-BMA (D) into rats bearing N1S1 orthotopic hepatocarcinoma. E: Contrast intensities of liver parenchyma, estimated using Image J software. (** $p < 0.01$, *** $p < 0.001$ with unpaired t-test between Gd-DTPA-pullulan and 0.05 mmol Gd/kg doase of Gd-DTPA-BMA).

a temperature of 22 ± 2 °C and a relative humidity of 55% ± 5%. Animal care and experimental procedures were performed in accordance with the guidelines issued by Inha University, School of Medicine, Animal Care and Use Committee.

Orthotopic HCC of rats was established in 8-week-old male Sprague Dawley rats. Briefly, 5×10^6 N1S1 hepatoma cells, routinely grown in RPMI 1640 medium supplemented with 10% fetal bovine serum (FBS), 100 IU/mL penicillin, 100 mg/mL streptomycin, and 2 mM L-glutamine in 5% CO_2 humidified air at 37 °C were inoculated into the terminal lobe of livers following laparotomy. Tumors were allowed to grow to reach a size of 200 to 400 mm^3 for MRI.

2.4.2. DEN induced cirrhotic HCC in rats

Most HCC occur secondary to viral hepatitis infection or cirrhosis. Cirrhotic HCC was induced using DEN (Sigma–Aldrich, St. Louis, MO, USA). DEN was diluted in the drinking water to a concentration of 100 mg/L and supplied to Sprague Dawley rats. Incidence and development of cirrhotic HCC were monitored based on histological assay of a control group which was undergoing the same treatment as the MRI test group. Rats with different stages of hepatic lesions (regenerative nodules and malignant HCC nodules) were subjected to MRI (Signa Excite; GE Healthcare, Milwaukee, WI, USA).

2.5. In vivo MRI

2.5.1. Conditions for MRI

MRI experiments were conducted on a 1.5-T horizontal scanner (Signa Excite; GE Healthcare) using a Litz Coil (diameter 100 mm, length 85 mm, DOTY Scientific Inc., NC, USA). The animals were anethesized by i.p. injection of cocktail soln. (ketamine, xylazine and acepromazine) and immobilized. Body temperature was maintained to be 37 °C with heating bed. T_1-weighted images were acquired pre- and post-contrast using the following parameters: fast spin echo, TR = 400.0 ms, TE = 10.0 ms and slice thickness = 3.0 mm.

2.5.2. In vivo MRI of HCC

Before the test, *in vivo* IV dose of Gd-DTPA-Pullulan to observe the *in vivo* MR sensitivity was adjusted on rat model. The optimal dose of Gd-DTPA-Pullulan and Gd-DTPA-BMA (Omniscan®, GE Healthcare) which was employed as a reference for the comparison was determined to be 0.05 mmol Gd/kg.

Gd-DTPA-Pullulan or Gd-DTPA-BMA was injected through a tail vein at a dose of 0.05 mmol Gd/kg. Rats with N1S1 orthotopic HCC or cirrhotic HCC were then immediately placed in a 1.5-T horizontal MR scanner (Signa Excite, GE Healthcare) and images were obtained at 0.1, 1, 3 and 24 h after injection and analyzed using Image J software.

2.6. Toxicity studies of Gd-DTPA-Pullulan

2.6.1. Cytotoxicity studies of Gd-DTPA-Pullulan

Cytotoxicities of Gd-DTPA-Pullulan, Gd-DTPA-BMA, and Gd-DTPA were estimated from Chang liver cells (human epithelial liver cells), which had been maintained in Eagle's Medium with Earle's BSS and 2 mM L-glutamine (EMEM) containing 10% fetal bovine serum, and 1% streptomycin-ampicillin under 5% CO_2 at 37 °C. Cells were seeded in 96-well plates at a density of 1000 cells per well, incubated for 24 h, and then treated with Gd-DTPA-Pullulan, Gd-DTPA-BMA, and Gd-DTPA. After 3 days of treatment, cell viability was determined using luminescent cell viability assay kit (CellTiter-Glo®, Promega, WI). Luminescence, produced by the luciferase-catalyzed reaction of luciferin and cellular ATP, was measured using a counter (Spectra Max M5, Molecular devices, CA). 100 μl CellTiter-Glo® was added to the well. After a 10 min of incubation at room temperature, the luminescent signal was recorded in counts per second.

2.6.2. Acute toxicity studies of Gd-DTPA-Pullulan

Acute toxicity of Gd-DTPA-Pullulan was evaluated based on histological observations of organs and plasma protein levels. Pathologic examinations of livers and kidneys were conducted 1 and 5 days after the rat tail-vein injections of Gd-DTPA-Pullulan (0.05 mmol Gd/kg). Livers and kidneys were dissected, fixed in 10% neutral buffered formalin (NBF), embedded in paraffin wax and further sliced and stained with hematoxylin and eosin (H&E) for microscopic observation.

Plasma levels of albumin (ALB), total bilirubin (T-BIL), alkaline phosphatase (ALP), aspartate aminotransferase (AST), alanine aminotransferase (ALT), gamma-glutamyl transferase (GGT), creatinine (CRE), and blood urea nitrogen (BUN) were measured. Briefly, Gd-DTPA-Pullulan was injected into Sprague Dawley rats at 0.05 mmol Gd/kg and 5 days later blood was sampled by cardiac puncture and collected in EDTA tubes. Plasma samples were separated by centrifugation at 2000 g for 10 min.

2.7. Urinary excretion of Gd-DTPA-Pullulan

Urinary excretion of Gd-DTPA-Pullulan was studied following an injection of 0.05 mmol Gd/kg to the tail vein of male Sprague Dawley rats. The rats were housed in metabolic cages, and urine samples were collected during the periods of 0–8, 8–24, 24–32, 32–48, and 48–72 h post injection. Food and water were supplied *ad*

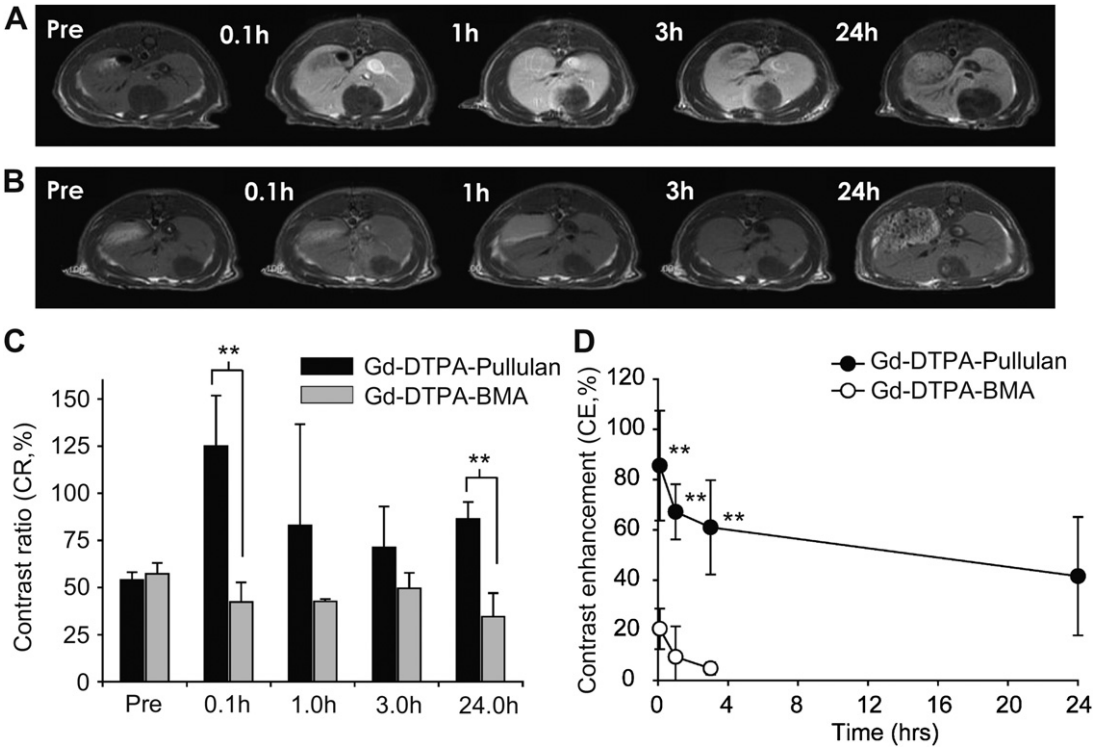

Fig. 4. A and B, time dependent MR images of HCC rats after I.V. injection of Gd-DTPA-Pullulan (A) and Gd-DTPA-BMA (B). C, contrast ratio (CR) of Gd-DTPA-Pullulan and Gd-DTPA-BMA, CR is the relative contrast of hepatic lesion to normal region. D, contrast enhancement (CE) of Gd-DTPA-Pullulan and Gd-DTPA-BMA, CE was calculated from the contrast-ratio of normal liver region between pre- and post- injection. Data are expressed as mean ± s.d. ($n = 4$), (** $p < 0.01$, *** $p < 0.001$ with unpaired t-test).

libitum during the experiment. The excreted amount of gadolinium was estimated using ICP-OES.

2.8. Tissue distribution of Gd-DTPA-Pullulan

Gd-DTPA-Pullulan and Gd-DTPA-BMA were injected into rats through a tail vein at a dose of 0.05 mmol Gd/kg. Rats were euthanized and tissue samples recovered 5 h post injection. The samples were washed with phosphate buffered saline (PBS), blotted with tissue-paper, weighed, and homogenized (Ultra-Turrax® T-25, IKA®, Germany) after dilution with PBS. A volume of 60% nitric acid was added to each sample and tissues were incubated for 2 days at 60 °C after which the solutions were centrifuged at 13,000 rpm for 30 min and the supernatant diluted with 3% ultra pure nitric acid and subjected to ICP-OES [24].

3. Results

3.1. Synthesis of Gd-DTPA-Pullulan

Fig. 2A and B shows the chemical structure of Gd-DTPA-Pullulan and the FT-IR spectra of pullulan, DTPA-Pullulan, and Gd-DTPA-Pullulan. We also illustrated the synthetic pathway of Gd-DTPA-Pullulan at Fig. S1. DTPA, as a gadolinium chelate residue, was chemically introduced to the hydroxyl groups of pullulan to prepare DTPA-pullulan, and Gd^{3+} was coordinated on the residue of DTPA (Fig. 2A). The formation of an ester bond between pullulan and DTPA was indicated by C═O and C–O stretching absorptions at 1736 and 1135 cm^{-1}, respectively. After introducing gadolinium to DTPA-pullulan, the typical peak of O–C═O$^-$ moved to 1712 and 1029 cm^{-1}, respectively because of coordination between the O–C═O$^-$ and Gd^{3+}. The formation of Gd-DTPA-pullulan was re-confirmed by measuring estimation zeta-potential. Briefly, pullulan, DTPA-pullulan, or GDP were dissolved in distilled water at a concentration of 10 mg/ml and transferred to a Zetasizer Nano (Malvern instruments Ltd, Worcestershire, UK). Zeta-potentials were determined by measuring electrophoretic mobilities. The zeta-potential of pullulan was -0.1 ± 0.43 mV and reduced to -14.3 ± 1.9 mV after the conjugation with DTPA. DTPA has five carboxylic acids (O–C═O–) and DTPA-conjugation modified the charge of pullulan from neutral to negative. Consequently, the negative charge of DTPA-pullulan shifted to -3.2 ± 1.5 mV after the introduction of Gd^{3+}. These results indicate that the O–C═O– residue of DTPA-pullulan coordinated with Gd^{3+} in Gd-DTPA-Pullulan.

3.2. In vitro paramagnetic properties of Gd-DTPA-Pullulan

In vitro paramagnetic properties of Gd-DTPA-Pullulan and Gd-DTPA-BMA were evaluated using a 1.5 MR scanner. Fig. 3A shows that Gd-DTPA-Pullulan exerted a much brighter contrast effect than Gd-DTPA-BMA at the same gadolinium concentration. The contrast intensities of phantom images, which were obtained by using Image J software, also supported the stronger paramagnetic properties of Gd-DTPA-Pullulan (Fig. 3B). Gd-DTPA-Pullulan displayed 5∼7 times higher contrast intensity than GD-DTPA-BMA at 0.0005 mM of Gd concentration. This increased MR sensitivity of Gd-DTPA-Pullulan is explained by the molecular structure of pullulan. Pullulan has many hydroxyl groups which attract water molecules, increase local water density, and consequently amplify the water exchange rate on gadolinium molecules, which induces high T_1 relaxivity [8,25–27].

3.3. Intravenous dosage adjustment of Gd-DTPA-Pullulan

For the dosage adjustment of Gd-DTPA-Pullulan, different doses (0.05, 0.025, and 0.0125 Gd mmol/kg for Gd-DTPA-Pullulan, 0.05 Gd mmol/kg for Gd-DTPA-BMA) were injected to rats via a tail vein, and MRI was performed (Fig. 3C–F). Contrast intensities of hepatic parenchyma increased in parallel with the intravenous dose of Gd-DTPA-Pullulan. The MR contrast intensity of Gd-DTPA-Pullulan was 1.63 times higher than that of Gd-DTPA-BMA at a dose of 0.05 mmol Gd/kg (Fig. 3G). Even a 0.0125 mmol Gd/kg dose of Gd-DTPA-Pullulan displayed a higher intensity than 0.05 mmol Gd/kg of Gd-DTPA-BMA. The effective reduced dose (one-eighth of the usual dose) of Gd-DTPA-Pullulan implies an increased safety window.

3.4. In vivo delayed hepatic MR images of orthotopic HCC

The results of the comparative *in vivo* MR study on Gd-DTPA-Pullulan and Gd-DTPA-BMA in our orthotopic HCC model are presented in Fig. 4. Histological examinations, performed after MRI, confirmed the formation of HCC and corresponded to MRI findings (Fig. S2). Contrast enhancement by Gd-DTPA-Pullulan was enough to differentiate malignant and normal regions in delayed MRI (Fig. 4A). Signal intensities in regions of interest (ROI) were measured using Image J software. Contrast ratios (CR) between malignant and normal regions on the same imaging frames were calculated using the following equation [28]:

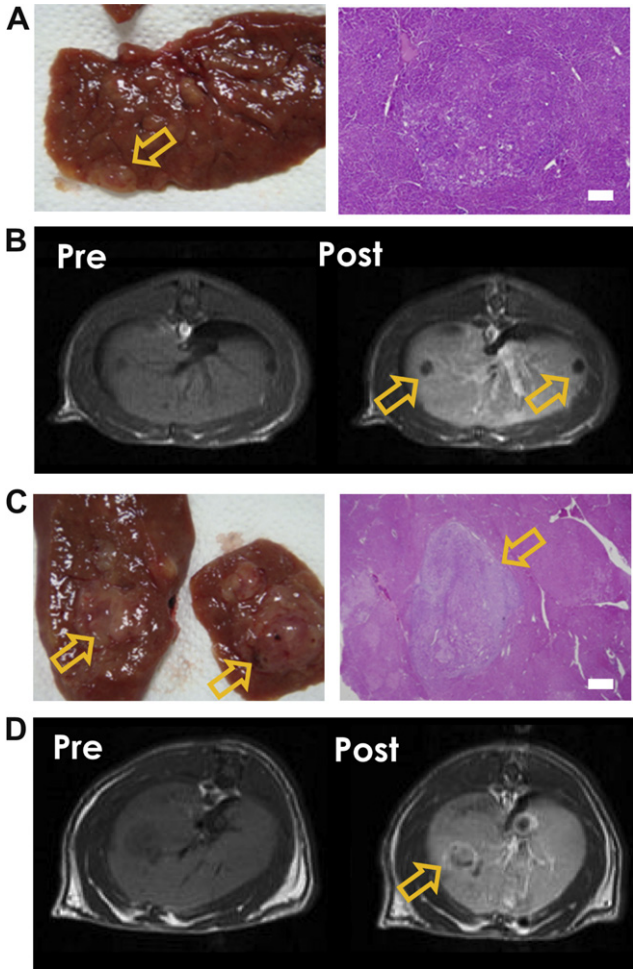

Fig. 5. T_1-weighted MR images and histologies of DEN-induced fibrotic cirrhosis (A and B) and cirrhotic HCC (C and D). Gd-DTPA-Pullulan detected nodules in both cirrhotic (B) and HCC nodules (D), whereas capsular bright contrast was observed on the malignant HCC nodules (D, arrow). Histologies confirmed typical characteristics of cirrhotic (A) and HCC nodules (B). Scale bar, 50 μm (For interpretation of the references to color in this figure legend, the reader is referred to the web version of this article.)

$$CR = \frac{Intensity_{liver} - Intensity_{tumor}}{Intensity_{tumor}} \times 100\%$$

Signal intensities of ROIs pre- and post-injection are presented as contrast enhancement (CE), calculated using the following equation [28]:

$$CE = \frac{Intensity_{post} - Intensity_{pre}}{Intensity_{pre}} \times 100\%$$

As shown in Fig. 4C and D, CR and CE increased by 124.8% and 80% immediately after injecting Gd-DTPA-Pullulan, and these values were almost 3 to 4 times higher than those of Gd-DTPA-BMA (124.0 ± 42.3 *vs.* 26.9 ± 10.4 for CR, 85.5 ± 20.6 *vs.* 21.8 ± 8.1 for CE). In particular, Gd-DTPA-Pullulan maintained contrast enhancement in ultra-delayed MRI up to 24 h after dosing (Fig. 3D, 41.5% of CE at 24 h).

3.5. In vivo MR images of DEN-induced HCC

Most hepatocarcinoma (HCC) develops from cirrhosis induced by chronic viral hepatitis and alcoholic liver. Regenerative nodules initially develop in cirrhotic liver which gradually progress to dysplastic nodules and then malignant HCC nodules. Cellular density, nodule size, and vascular density increase with the progress of HCC [29,30]. Typically, regenerative nodules develops in 6–7 weeks after DEN treatment (Fig. 5A) and cirrhotic HCC is observed several weeks later (Fig. 5C). N1S1 forms a single massive HCC with a distinct margin which is easily detected by MRI (Fig. S2B), whereas cirrhotic HCC is surrounded by fibrous capsules with an indistinct margin making it difficult to differentiate the hepatic lesions.

Our Gd-DTPA-Pullulan showed the enhanced and discriminative MR contrast on the initially developing regenerative nodules (Fig. 5B) and malignant HCC nodules (Fig. 5D). Interestingly, malignant nodules showed contrast enhancement on the capsular boundary of nodules, probably from the preferential accumulation of Gd-DTPA-Pullulan on the surrounding boundary of nodules. We assume that newly formed arteries facilitated the accumulation of Gd-DTPA-Pullulan, inducing this regional enhancement.

3.6. The toxicities of Gd-DTPA-Pullulan

We evaluated the cytotoxicities of Gd-DTPA-Pullulan, Gd-DTPA-BMA, and Gd-DTPA on Chang liver cells (human epithelial liver cells). The IC_{50} (50% inhibition concentration) values of Gd-DTPA-Pullulan and Gd-DTPA-BMA were 309.1 ± 11.2 μM and 49.4 ± 8.9 μM, respectively, whereas that of Gd-DTPA was 173.5 ± 15.5 μM (Fig. 6A). Cytotoxicity of Gd-DTPA-Pullulan is approximately 6 times lower than that of Gd-DTPA-BMA in Chang liver cells. Histology of liver and kidney samples were observed 1 and 5 days after Gd-DTPA-Pullulan administration (Fig. 6B). At these times, hepatocytes and other liver cells appeared normal, and no signs of necrosis, inflammatory cell infiltration, or hepatocyte swelling were detected. Histologically, kidney sections also appeared normal with no evidence of tubular epithelium degeneration, hemorrhage, or fibrosis. Furthermore,

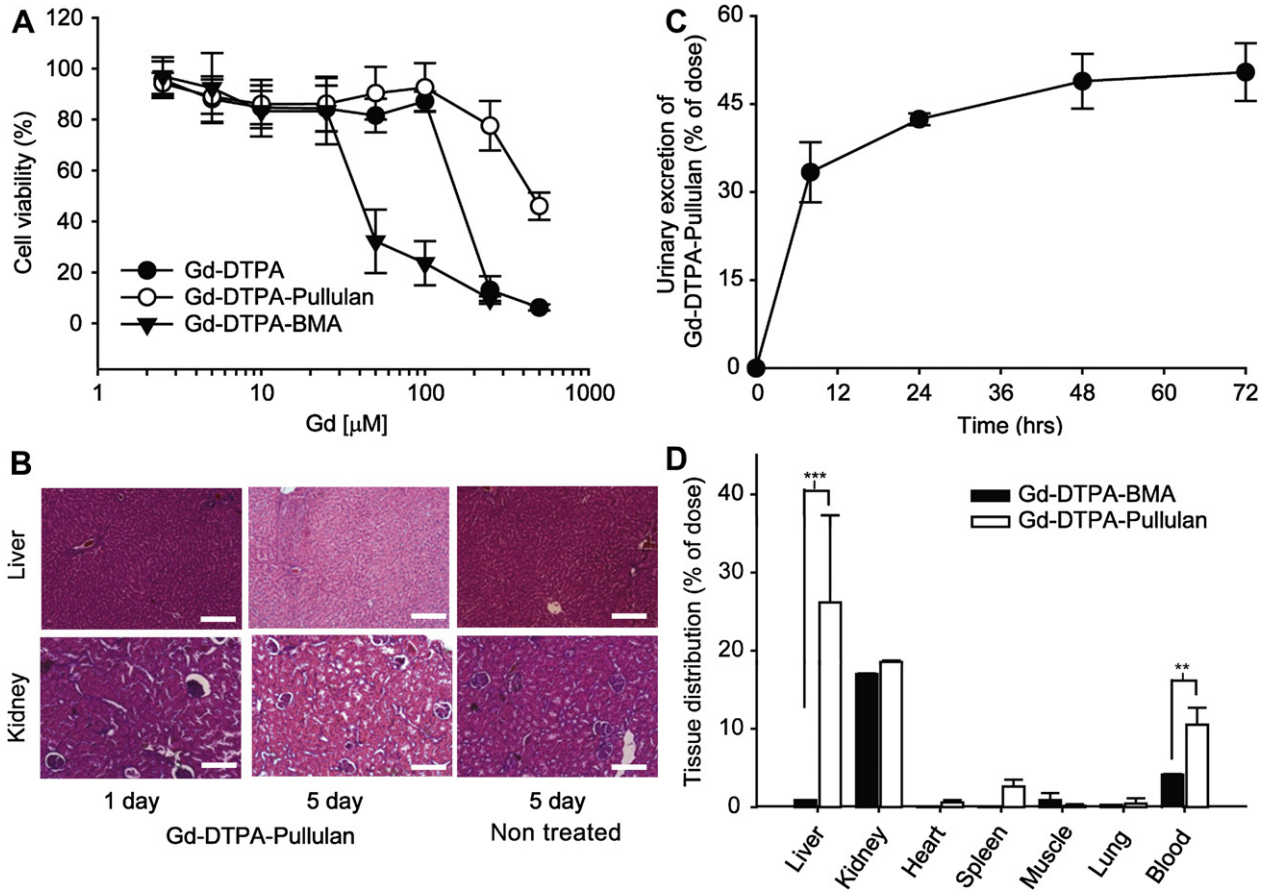

Fig. 6. A, viabilities of Chang liver cells after treatment of Gd-DTPA-Pullulan, Gd-DTPA-BMA, Gd-DTPA. B, H&E stained liver and kidney tissues. Tissues were recovered 1 and 5 days after an I.V. injection of Gd-DTPA-Pullulan at a dose of 0.05 mmol Gd/kg. C, urinary excretion rate of Gd-DTPA-Pullulan in rats. D, tissue distribution of Gd-DTPA-Pullulan and Gd-DTPA-BMA, tissues were recovered after 5 h of I.V. injection, and analyzed on a ICP-OES. Data are expressed as mean ± s.d. ($n = 4$), ($^{**}p < 0.01$, $^{***}p < 0.001$ with unpaired *t*-test). Scale bar, 200 μm.

plasma protein levels were not different between Gd-DTPA-Pullulan treated rats and non-treated rats (Table 1).

3.7. Excretion and tissue distribution of Gd-DTPA-Pullulan

Most gadolinium chelates are excreted rapidly, primarily via the kidneys. In particular, up to 94% of Gd-DTPA-BMA administered to rats is excreted in this manner, and only 1–4% is excreted via the hepatobiliary system [31]. Our tissue distribution studies, performed 5 hrs post-injection, showed that approximately 26.2% of Gd-DTPA-Pullulan stayed in the liver, whereas only 0.89% of Gd-DTPA-BMA remained (Fig. 6D). Urinary elimination studies, which were performed for 72 hrs after intravenous injection, showed that 50.4% of Gd-DTPA-Pullulan was eliminated via the urine (Fig. 6C). These results highly agree with reported pharmacokinetic studies, which determined that 40 ~ 50% of pullulan was retained in the liver and excreted via the biliary pathway [19,21]. Our study also supported billiary elimination of Gd-DTPA-Pullulan is much higher than that of Gd-DTPA-BMA during the 5 h after injection (Fig. S4).

4. Discussion

Presently, most cancer therapy, including diagnosis, location of metastases, drug regimens, and determination of surgical margin, is becoming more reliant than ever on imaging technologies [1,2]. Magnetic resonance imaging (MRI) provides the most discriminative diagnostic images on soft tissues than any other technologies do. MRI technology allows physicians to accurately and non-invasively diagnose many pathologies [32].

In this present study, we designed pullulan attached Gd-DTPA as a hepatocyte-specific gadolinium chelate to achieve high MR contrast. Gd-DTPA-Pullulan provided enhanced (67.1% CE after 1 h) and sustained (41.5% CE at 24 h) contrast following injection. In comparison, Gd-DTPA-BMA showed only 9.4% CE 1 h after injection (Fig. 4D).

This enhanced MR contrast can be explained by the typical properties of pullulan. Gadolinium chelates generate contrast by lowering the spin-lattice relaxation time of nearby water protons. Pullulan has abundant hydroxyl groups which increase the local density of water molecules, amplify the water exchange rate on gadolinium molecules, consequently enhancing the longitudinal water proton relaxation rate [8,25–27].

Preferential accumulation of Gd-DTPA-Pullulan in the liver could be another explanation for the enhancement of hepatic MR contrast. Gd-DTPA-Pullulan accumulates in the liver with a longer residence time, which consequently prolongs the contrast enhancement in delayed hepatic MRI up to 24 h after injection. Pullulan leads the hepatocyte-specific uptake of gadolinium via asialoglycoprotein receptors. Recently, the elongated MR contrast time on liver MR imaging has been reported. Most of them are using nano-carries, such as liposomes, micelles, dendrimers and etc., which are accumulated on liver via hepatic RES system [14,33,34]. Chen et al. achieved the lasting MR contrast for 4.5 hrs after an injection of gadolinium which was conjugated with PLA-PEG-DTPA nanoparticles [35]. But their system, although gadolinium was applied, also seem to be a RES-specific agent rather hepatocyte-specific agent. Fig. S3 shows the cytosolic residence of Gd-DTPA-Pullulan (Red fluorescence from RITC attached Gd-DTPA-Pullulan) which come from the uptake of Gd-DTPA-Pullulan by hepatocytes.

Mn-DPDP (Manganese dipyroxyl diphosphate, Teslascan®, GE Healthcare), a typical hepatocyte-specific T_1 agent, sustained the contrast to the same degree from 5 to 120 min [36]. Gd-DTPA-BMA provides less than 30 min of diagnostic time which is not always enough to obtain clear and discriminative hepatic imaging. So, ultra-delayed hepatic diagnostic time of Gd-DTPA-Pullulan up to 24 h could be considered another clinical improvement with regard to hepatic MRI. Furthermore, acute toxicity studies implied Gd-DTPA-Pullulan might be a safe and eligible MR contrast agent for further development and clinical applications (Table 1, Fig. 6A and B).

Table 1
Effect of Gd-DTPA-Pullulan on liver and kidney functions in rats after i.v. injection at a dose of 0.05 mmol Gd/kg.

	Gd-DTPA-Pullulan	Non treated	*P* value[a]
ALB	2.33 ± 0.21	2.5 ± 0.06	0.18
T-BIL	0.01 ± 0.02	0.00 ± 0.00	0.25
ALP	406.67 ± 127.99	637.00 ± 7.45	0.05
AST	130.33 ± 30.09	144.67 ± 19.55	0.53
ALT	50.67 ± 9.07	69.67 ± 13.31	0.11
GGT	0.67 ± 0.58	0.00 ± 0.06	0.37
CRE	0.56 ± 0.01	0.55 ± 0.01	1.00
BUN	14.13 ± 0.55	15.33 ± 3.23	0.56
LDH	1064.00 ± 659.57	1786.67 ± 502.34	0.21

[a] *P* values were obtained from *t*-test, ALB; albumin, T-BIL; total bilirubin, ALP; alkaine phosphatease, AST; aspartate aminotransferase, ALT; alanine aminotransferase, GGT; gammaglutamyl transferase, CRE; creatinine, creatinine, BUN; blood urea nitrogen, LDH; lactate dehydrogenase. Data are expressed as mean ± s.d. ($n = 3$).

5. Conclusion

A new hepato-specific MR contrast agent (Gd-DTPA-Pullulan) was successfully synthesized and subjected to preclinical and functional evaluation. Gd-DTPA-Pullulan provided enhanced contrast of hepatic parenchyma in delayed MRI, with discriminative contrast power in relation to cirrhotic HCC. Pharmacokinetic evaluation showed Gd-DTPA-Pullulan highly accumulates in the liver which suggests Gd-DTPA-Pullulan is working as a hepatocyte-specific MR contrast agent.

Acknowledgements

This research was financially supported by the Fundamental R&D Program for Core Technology of Materials, Republic of Korea, the Gyeonggi Regional Research Center (GRRC), the Ministry of Knowledge Economy (MKE), and the Korea Industrial Technology Foundation (KOTEF) through the Human Resource Training Project for Strategic Technology, by the Catholic University of Korea, Research Fund, 2011.

Appendix. Supplementary data

Supplementary data associated with this article can be found in the online version, at doi:10.1016/j.biomaterials.2011.03.069.

References

[1] Koh DM, Cook GJ, Husband JE. New horizons in oncologic imaging. N Engl J Med 2003;348:2487–8.
[2] Weissleder R. Molecular imaging in cancer. Science 2006;312:1168–71.
[3] Heiken J, Weyman P, Lee J, Balfe D, Picus D, Brunt E, et al. Detection of focal hepatic masses: prospective evaluation with CT, delayed CT, CT during arterial portography, and MR imaging. Radiology 1989;171:47–51.
[4] Rofsky N, Weinreb J, Bernardino M, Young S, Lee J, Noz M. Hepatocellular tumors: characterization with Mn-DPDP-enhanced MR imaging. Radiology 1993;188:53–9.
[5] Matsui O, Kadoya M, Kameyama T, Yoshikawa J, Takashima T, Nakanuma Y, et al. Benign and malignant nodules in cirrhotic livers: distinction based on blood supply. Radiology 1991;178:493–7.
[6] Semelka R, Helmberger T. Contrast agents for MR imaging of the liver. Radiology 2001;218:27–38.
[7] Sitharaman B, Van Der Zande M, Ananta JS, Shi X, Veltien A, Walboomers XF, et al. Magnetic resonance imaging studies on gadonanotube-reinforced

biodegradable polymer nanocomposites. J Biomed Mater Res A 2010;93:1454–62.
[8] Pierre VC, Botta M, Raymond KN. Dendrimeric gadolinium chelate with fast water exchange and high relaxivity at high magnetic field strength. J Am Chem Soc 2005;127:504–5.
[9] Grange C, Geninatti-Crich S, Esposito G, Alberti D, Tei L, Bussolati B, et al. Combined delivery and magnetic resonance imaging of neural cell adhesion molecule-targeted doxorubicin-containing liposomes in experimentally induced Kaposi's sarcoma. Cancer Res 2010;70:2180–90.
[10] Corot C, Robert P, Lancelot E, Prigent P, Ballet S, Guilbert I, et al. Tumor imaging using P866, a high-relaxivity gadolinium chelate designed for folate receptor targeting. Magn Reson Med 2008;60:1337–46.
[11] Shu CY, Ma XY, Zhang JF, Corwin FD, Sim JH, Zhang EY, et al. Conjugation of a water-soluble gadolinium endohedral fulleride with an antibody as a magnetic resonance imaging contrast agent. Bioconjug Chem 2008;19:651–5.
[12] Chen W, Vucic E, Leupold E, Mulder WJ, Cormode DP, Briley-Saebo KC, et al. Incorporation of an apoE-derived lipopeptide in high-density lipoprotein MRI contrast agents for enhanced imaging of macrophages in atherosclerosis. Contrast Media Mol Imaging 2008;3:233–42.
[13] Geninatti Crich S, Bussolati B, Tei L, Grange C, Esposito G, Lanzardo S, et al. Magnetic resonance visualization of tumor angiogenesis by targeting neural cell adhesion molecules with the highly sensitive gadolinium-loaded apoferritin probe. Cancer Res 2006;66:9196–201.
[14] Swanson SD, Kukowska-Latallo JF, Patri AK, Chen C, Ge S, Cao Z, et al. Targeted gadolinium-loaded dendrimer nanoparticles for tumor-specific magnetic resonance contrast enhancement. Int J Nanomed 2008;3:201–10.
[15] Reimer P. Tumor-targeted MR contrast agents: hype or future hope? Radiology 2004;231:1–2.
[16] Bellin M. MR contrast agents, the old and the new. Eur J Radiol 2006;60:314–23.
[17] Gandhi SN, Brown MA, Wong JG, Aguirre DA, Sirlin CB. MR contrast agents for liver imaging: what, when, how. Radiographics 2006;26:1621–36.
[18] Weinmann HJ, Ebert W, Misselwitz B, Schmitt-Willich H. Tissue-specific MR contrast agents. Eur J Radiol 2003;46:33–44.
[19] Rekha M, Sharma C. Pullulan as a promising biomaterial for biomedical applications: a perspective. Trends Biomater Artif Organ 2007;20:116–21.
[20] Trere D, Fiume L, De Giorgi LB, Di Stefano G, Migaldi M, Derenzini M. The asialoglycoprotein receptor in human hepatocellular carcinomas: its expression on proliferating cells. Br J Cancer 1999;81:404–8.
[21] Yamaoka T, Tabata Y, Ikada Y. Body distribution profile of polysaccharides after intravenous administration. Drug Delivery 1993;1:75–82.
[22] Caravan P, Ellison JJ, McMurry TJ, Lauffer RB. Gadolinium(III) Chelates as MRI contrast agents: structure, dynamics, and applications. Chem Rev 1999;99:2293–352.
[23] Hosseinkhani H, Hosseinkhani M. Biodegradable polymer-metal complexes for gene and drug delivery. Curr Drug Saf 2009;4:79–83.
[24] Feng Y, Zong Y, Ke T, Jeong EK, Parker DL, Lu ZR. Pharmacokinetics, biodistribution and contrast enhanced MR blood pool imaging of Gd-DTPA cystine copolymers and Gd-DTPA cystine diethyl ester copolymers in a rat model. Pharm Res 2006;23:1736–42.
[25] Caravan P, Astashkin AV, Raitsimring AM. The gadolinium(III)-water hydrogen distance in MRI contrast agents. Inorg Chem 2003;42:3972–4.
[26] Caravan P. Strategies for increasing the sensitivity of gadolinium based MRI contrast agents. Chem Soc Rev 2006;35:512–23.
[27] Werner EJ, Datta A, Jocher CJ, Raymond KN. High-relaxivity MRI contrast agents: where coordination chemistry meets medical imaging. Angew Chem Int Ed Engl 2008;47:8568–80.
[28] Marchal G, Zhang X, Ni Y, Van Hecke P, Yu J. AL.B. Comparison between Gd-DTPA, Gd-EOB-DTPA, and Mn-DPDP in induced HCC in rats: a correlation study of MR imaging, microangiography, and histology. Magn Reson Imaging 1993;11:665–74.
[29] Bonekamp S, Kamel I, Solga S, Clark J. Can imaging modalities diagnose and stage hepatic fibrosis and cirrhosis accurately? J Hepatol 2009;50:17–35.
[30] El-Serag HB, Rudolph KL. Hepatocellular carcinoma: epidemiology and molecular carcinogenesis. Gastroenterology 2007;132:2557–76.
[31] Kindberg GM, Uran S, Friisk G, Martinsen I, Skotland T. The fate of Gd and chelate following intravenous injection of gadodiamide in rats. Eur J Radiol 2010;20:1636–43.
[32] Moonen CT, van Zijl PC, Frank JA, Le Bihan D, Becker ED. Functional magnetic resonance imaging in medicine and physiology. Science 1990;250:53–61.
[33] Lipinski MJ, Amirbekian V, Frias JC, Aguinaldo JG, Mani V, Briley-Saebo KC, et al. MRI to detect atherosclerosis with gadolinium-containing immunomicelles targeting the macrophage scavenger receptor. Magnet Reson Med 2006;56:601–10.
[34] Erdogan S, Torchilin VP. Gadolinium-loaded polychelating polymer-containing tumor-targeted liposomes. Methods Mol Biol 2010;605:321–34.
[35] Chen Z, Yu D, Liu C, Yang X, Zhang N, Ma C, et al. Gadolinium-conjugated PLA-PEG nanoparticles as liver targeted molecular MRI contrast agent. J Drug Target; 2010:1–9.
[36] Tanimoto A, Kreft BP, Baba Y, Zhao L, Finn JP, Compton CC, et al. Evaluation of hepatocyte-specific paramagnetic contrast media for MR imaging of hepatitis. J Magn Reson Imaging 1993;3:786–93.